ESO-Based Safety-Critical Control for Robotic Systems With Unmeasured Velocity and Input Delay

Sihua Zhang, Di-Hua Zhai, Juncheng Lin, Yuhan Xiong, Yuanqing Xia, *Senior Member, IEEE*, and Minfeng Wei

***Abstract*—For practical robots, obtaining precise dynamic models and states is a challenge, which presents difficulty in achieving safety-critical control. When faced with an uncertain dynamic model of the robotic system and the absence of measurements for joint velocity, this article proposes a method by combining extended state observer (ESO) and control barrier function (CBF) for safety-critical control. Firstly, an ESO is used to estimate the model and states in real time. Then, according to the estimation error, the ESO-based CBF (ESO-CBF) is proposed, and a quadratic programming subject to ESO-CBF is constructed to calculate the control input for robotic systems. In addition, input delay is also considered for robotic systems with uncertain models. In cases involving input delay, a predictive ESO is designed to estimate the model, and the corresponding estimation error boundary is derived. Based on the estimation error, ESO-CBF is constructed to ensure the safety constraint. Finally, the effectiveness of the proposed method is verified by the obstacle avoidance task of Franka Emika Panda manipulator.**

***Index Terms*—Control barrier function (CBF), extended states observer (ESO), input delay, robotic systems, uncertainty.**

I. Introduction

THE use of robotic systems, including industrial robots and UAVs, has become widespread in both production and daily life [1]. One crucial aspect of these applications is ensuring safety, especially in scenarios involving human–robot interaction or navigating within multirobot systems to prevent collisions. Therefore, the design of a dependable safety-critical controller has paramount significance.

In the field of control systems, safety is typically approached by formulating it as a problem of set forward invariance, which requires the system's states to remain within a safe set at all times. A solution to this problem is proposed in [2] through the theory of control barrier function (CBF), which has been extensively studied for dynamic systems with accurate models and measurable states [3], [4], [5], [6]. However, obtaining accurate dynamic models for robotic systems can be difficult, and joint velocity sensors may be absent in many industrial robotic systems, with added velocity sensors being prone to errors due to noise [7]. In addition, uncertain factors like communication delays can result in delays in control input execution [8], which can negatively impact both control performance and safety guarantees [9]. To address these challenges, this article aims to achieve safety-critical control of robotic systems in the presence of model uncertainty, unmeasured joint velocity, and input delay.

For systems with uncertain models, various methods have been proposed to guarantee safety using CBF. In [10], robust CBF provided robustness against uncertainty and is suitable for cases where the model uncertainty is independent of the control input, and the boundaries of uncertainty are known. Adaptive CBF and robust adaptive CBF were proposed in [11] and [12] for safety-critical control of systems with unknown model parameters. In addition to these model-based approaches, data-driven methods such as Gaussian process [13] and neural network [14] have been used to learn the uncertainty in systems. The CBF conditions are then constructed based on the learned model to ensure safety. However, these methods typically require access to perfect state information, which is often not available in practical systems. In most instances, the true system state is unknown and must be reconstructed using measurements from sensors, which may introduce noise. The utilization of imperfect state information can potentially lead to safety violations.

Recently, there has been increased attention given to the important problem of ensuring safety in systems with imperfect state information. In [15], measuring robust CBF was proposed for guaranteeing safety in output-feedback, in the

Manuscript received 1 May 2023; revised 22 July 2023, 26 September 2023, 21 November 2023, and 19 December 2023; accepted 24 December 2023. This work was supported in part by the National Natural Science Foundation of China under Grant 62173035, Grant 61803033, and Grant 61836001, in part by the "Xiaomi Young Scholars" from Xiaomi Foundation, and in part by the BIT Research and Innovation Promoting Project under Grant 2023YCXY035. *(Corresponding author: Di-Hua Zhai.)*

Sihua Zhang, Juncheng Lin, Yuhan Xiong, Yuanqing Xia, and Minfeng Wei are with the School of Automation, Beijing Institute of Technology, Beijing 100081, China (e-mail: sihua.zhang@bit.edu.cn; 3120210946@bit.edu.cn; 3120200964@bit.edu.cn; xia_yuanqing@bit.edu.cn; 3220185079@bit.edu.cn).

Di-Hua Zhai is with the School of Automation, Beijing Institute of Technology, Beijing 100081, China, and also with the Yangtze Delta Region Academy of Beijing Institute of Technology, Jiaxing 314001, China (e-mail: zhaidih@bit.edu.cn).

Color versions of one or more figures in this article are available at https://doi.org/10.1109/TIE.2024.3349592.

Digital Object Identifier 10.1109/TIE.2024.3349592

context of vision-based control. The authors made assumptions about noiseless sensors and the availability of an imperfect inverse of the measurement map. Consequently, from a single measurement, a ball enclosing the true state can be determined. However, the applicability of this method is constrained by the challenge of obtaining the Lipschitz constant of the system model, which is a prerequisite for its implementation. Furthermore, it is common practice to design full-state feedback controllers and subsequently replace the state with an estimate provided by an observer in system designs. Consequently, observers-based CBF emerges as an alternative to ensuring safety. In [16], a safety-critical controller was proposed for stochastic systems, offering a probabilistic assurance of safety. The authors considered linear measurement maps, additive Gaussian disturbances, and specifically employed the extended Kalman filter as the observer. This work was further extended in [17] to encompass a broader class of control-affine systems, enabling probabilistic safety guarantees over a finite forward interval. Nevertheless, establishing safety deterministically remains a challenging task.The authors in [18] proposed two approaches to synthesize observer–controller interconnections to deterministically guarantee safety. The first approach utilizes input-to-state stable observers, and the second uses bounded error observers. By using the boundary of observation error and the Lipschitz constant of the safety constraint, two observer-based CBF methods are constructed. However, obtaining the Lipschitz constant of the safety constraint can pose difficulties in certain cases, limiting the practicality of this method. In [19], the authors introduced a robust CBF by altering the conditions related to the Lipschitz constant of a CBF in [18] to be based on the boundary of the safety constraint's derivative. However, determining this boundary becomes challenging, particularly when dealing with complex constrained functions and high-dimensional states in robotic systems. In this article, an observer-based CBF is proposed to deterministically guarantee safety in robotic systems with uncertainty and partially available state information. This method relies solely on the estimation error, providing a means to ensure safety in robotic systems.

Moreover, recent literature has witnessed a growing emphasis on ensuring the safety of input delay systems. Specifically, [20] and [21] have proposed safety-critical control methods for linear and nonlinear continuous-time systems with input delay, while [22] has studied discrete-time control systems with input delays. However, these approaches rely on predicting future states, thereby introducing the potential for errors and violations of safety constraints when the system model is uncertain. To address this limitation, [23] introduced a robust method against prediction errors. Nevertheless, this approach requires knowledge of the boundary of prediction error and the Lipschitz constant of the system model, which can prove challenging to acquire in the context of robotic systems characterized by uncertain models. To overcome this issue, a predictive observer is presented in this article to account for both model uncertainty and input delay. Furthermore, CBF is improved based on the estimation error to ensure safety. By incorporating the predictive observer and considering the estimation error, this method provides a more reliable approach to guarantee safety in robotic systems with uncertain models and input delays.

Given the popularity of the extended state observer (ESO) in designing control systems for uncertain systems, as it allows for real-time estimation of states, external disturbances, and nonlinear uncertain dynamics [24], this article focuses on an ESO-based estimation method for unknown dynamic models and joint velocities of robotic systems. A safety-critical controller is then developed based on this approach. The main contributions of this article are summarized as follows.

1) The article presents the concept of ESO-based CBF (ESO-CBF), a safety-critical control approach specifically designed for robotic systems with model uncertainty and unmeasured states. This approach relies solely on the estimation error of ESO, making it a more reliable solution for ensuring safety in such systems.
2) A predictive ESO (PESO) is designed to estimate the model uncertainty for robotic systems with input delay. Based on the boundary of estimation error, ESO-CBF is constructed to achieve safety-critical control.
3) The effectiveness of this approach is verified through the obstacle avoidance experiment of a Franka Emika Panda manipulator.

II. Preliminaries

A. Control Barrier Function

Consider an affine control system

$$\dot{x} = f(x) + g(x)u \tag{1}$$

where $x \in \mathbb{R}^n$, the drift term $f : \mathbb{R}^n \to \mathbb{R}^n$ and the input gain $g : \mathbb{R}^n \to \mathbb{R}^{n\times p}$ are locally Lipschitz continuous functions. For any initial state $x(t_0) \in \mathbb{R}^n$, $x(t)$ is the unique solution to system (1) on a maximum time interval $I(x_0) = [t_0, T_{\max})$. $u \in U \subset \mathbb{R}^p$ is the control input. U denotes the input constraint set and satisfies

$$U = \{u \in \mathbb{R}^p : u_{\min} \le u \le u_{\max}\}. \tag{2}$$

Given a closed set C defined by a continuous differentiable function $h(x) : \mathbb{R}^n \to \mathbb{R}$ as

$$C = \{x \in \mathbb{R}^n : h(x) \ge 0\}. \tag{3}$$

It is assumed that C is nonempty and has no isolated point. If for every $x_0 \in C$, the state $x(t)$ always stays in the set C for $t \in I(x_0)$, the set C is forward invariant [25]. Then, the safety of system (1) is guaranteed and the set C is called safe set.

To ensure set invariance, the CBF is derived. First, some important definitions are introduced.

Definition 1 ([26]): A continuous function $\alpha : [0, a) \to [0, \infty), a > 0$, is a class $\mathcal{K}$ function if it is strictly increasing and $\alpha(0) = 0$.

Definition 2 ([26]): For a continuous differentiable function $h(x) : \mathbb{R}^n \to \mathbb{R}$ with respect to system (1), the relative degree is the number of times it needs to be differentiated along with its dynamics until the control input explicitly shows in the corresponding derivative.

Suppose that the relative degree of function $h(x)$ is m, and the inequality $h(x) \geq 0$ is used as a constraint with the relative degree of m. If $m = 1$, the definition of CBF is given.

Definition 3: Given a set C as in (3), $h(x)$ is a CBF for system (1) if there exists a class $\mathcal{K}$ function $\alpha(\cdot)$ such that

$$\sup_{u \in U}[L_f h(x) + L_g h(x)u + \alpha(h(x))] \geq 0, \forall x \in C. \quad (4)$$

If $h(x)$ is a CBF, the admission set of control input is defined as $K_{cbf}(x) = \{u \in U : L_f h(x) + L_g h(x)u + \alpha(h(x)) \geq 0\}$. The following lemma guarantees the set C is forward invariant.

Lemma 1 ([4]): Given the set C defined by (3) for a continuous differentiable function $h(x)$, if $h(x)$ is a CBF, then Lipschitz continuous control input $u(t) \in K_{cbf}(x)$ renders the set C forward invariant.

B. High Order CBF

If the relative degree of $h(x)$ satisfies $m > 1$, the CBF cannot be used to guarantee the forward invariance of set since the control input u is no longer exhibited in (4). Therefore, the high order control barrier function (HOCBF) is proposed. A sequence of functions $\psi_i(x) : \mathbb{R}^n \to \mathbb{R}, i \in \{0, \ldots, m\}$ is first defined as $\psi_0(x) = h(x)$, $\psi_i(x) = \dot{\psi}_{i-1}(x) + \alpha_i(\psi_{i-1}(x))$ for $i \in \{1, \ldots, m\}$, where $\alpha_i(\cdot)$ denotes $(m-i)^{th}$ order differentiable class $\mathcal{K}$ function. A sequence of sets $C_i, i \in \{1, \ldots, m\}$ is then defined in the form of $C_i = \{x \in \mathbb{R}^n : \psi_{i-1}(x) \geq 0\}, i \in \{1, \ldots, m\}$. Given the functions $\psi_i(x) : \mathbb{R}^n \to \mathbb{R}, i \in \{0, \ldots, m\}$, the definition of HOCBF is as below.

Definition 4 ([27]): A function $h(x) : \mathbb{R}^n \to \mathbb{R}$ is a HOCBF of relative degree m for system (1) if there exist $(m-i)th$ order differentiable class $\mathcal{K}$ functions $\alpha_i, i \in \{1, \ldots, m-1\}$, and a class $\mathcal{K}$ function α_m such that

$$\sup_{u \in U}[\dot{\psi}_{m-1}(x) + \alpha_m(\psi_{m-1}(x))] \geq 0 \quad (5)$$

for all $x \in C_1 \cap \cdots \cap C_m$. Eq. (5) equals to $\psi_m(x) \geq 0$.

Similar to Lemma 1, the following result also guarantees the forward invariance of set C.

Lemma 2 ([27]): The set $C_1 \cap \cdots \cap C_m$ is forward invariant for system (1) if $x(0) \in C_1 \cap \cdots \cap C_m$ and $h(x)$ is a HOCBF.

C. Optimal Control With CBF

For system (1) with states constraint, the control input is usually solved point-wise, where the time interval $[0, T]$ is divided into a finite number of intervals $[t_k, t_{k+1}), k = 0, 1, 2 \ldots n$. Besides, the constraint is linear in control and the states are fixed at each interval, so that a quadratic programming (QP) as follows is constructed to get the control input at each interval.

$$\begin{aligned} u^* &= \arg\min_u \|u - u_{nom}\|^2 \\ \text{s.t.} \quad & L_f h(x) + L_g h(x)u + \alpha(h(x)) \geq 0, \\ & u_{\min} \leq u \leq u_{\max} \end{aligned} \quad (6)$$

where u_{nom} is a nominal feedback controller. When $u_{nom} \notin K_{cbf}(x)$, the CBF constraint will minimally modify the nominal controller to ensure safety. The whole process of solving the optimal control problem with CBF constraint to guarantee the safety is shown in Fig. 1.

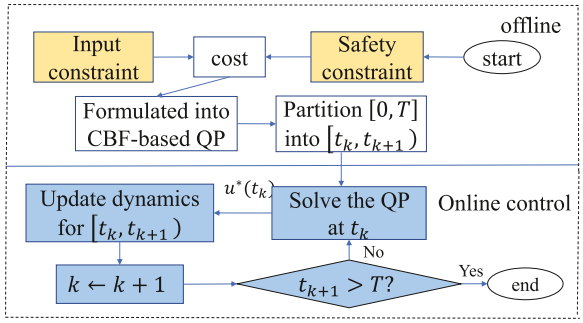

Fig. 1. Flowchart for solving a CBF constrained optimal control problem.

Remark 1: Noted that this method works conditioned on the fact that the QP (6) at every time interval is feasible. Some methods can be used to guarantee the feasibility of QP (6). The authors in [28] introduced adaptive CBF to resolve the conflict between CBF constraint and input constraint by introducing penalty functions in the definition of CBF and defining auxiliary dynamics for these penalty functions.The authors in [29] provided a method to find sufficient conditions to guarantee the feasibility of QP subject to CBF constraint and input constraint. Based on the above methods, the feasibility of QP (6) can be guaranteed. Moreover, they are also easily implemented in QP (6). In this case, given that the feasibility of QP is not the focus of this article, it will not be analyzed in depth to present proposed control framework as concisely as possible.

III. Problem Statement

In practical robot applications, meeting the necessary conditions for ensuring the safety guarantee provided by the CBF-QP (6) control input u^* can be challenging. The challenges involve: 1) perfect state information: It can be difficult to obtain precise and whole states in practical scenarios. While joint angle measurements are feasible, velocity sensors may be lacking in some commercial robots, leading to inaccuracies in states; 2) precise model of the system: The dynamic model of the robotic system can be subject to uncertainty due to unknown structural parameters or the presence of disturbances. This uncertainty further complicates the safety assurance; 3) implementing the control input perfectly: Actuator limitations always exists in practice. Moreover, when the controller is interconnected with the robotic system via communication networks, communication delays may arise, affecting the overall system performance.

To address these challenges and ensure the safety of the robotic system, this section introduces some assumptions and mathematical descriptions of these problems.

For a rigid n-link robotic system, the true dynamic model is expressed as

$$M(q)\ddot{q} + C(q, \dot{q})\dot{q} + G(q) + f_{dis} = u \quad (7)$$

where $q, \dot{q}, \ddot{q} \in \mathbb{R}^n$ denote the angle, velocity, and acceleration of joint, respectively. $M(q) \in \mathbb{R}^{n\times n}$, $C(q,\dot{q}) \in \mathbb{R}^{n\times n}$, and $G(q) \in \mathbb{R}^n$ are inertia matrix, Coriolis-centrifugal matrix, and gravitational term, respectively. f_{dis} denotes the bounded and continuous differentiable external disturbances. The system (7) possesses the following properties [30].

Property 1: The matrix $M(q)$ is uniformly positive definite and there exist two positive constants μ_1, μ_2 such that $0 < \mu_1 I_n \leq M(q) \leq \mu_2 I_n$, where I_n is an identity matrix.

Property 2: $\exists g_b, c_b \in \mathbb{R}^+$ such that $\|G(q)\| \leq g_b$ and $\|C(q,\dot{q})\| \leq c_b\|\dot{q}\|$.

Due to the existence of external disturbances, the dynamic model is not precisely known. Define $x = [q^T, \dot{q}^T]^T$, when $\dot{q}$ is unmeasured, (7) is expressed as

$$\dot{x} = \begin{bmatrix} I_n \\ 0_n \end{bmatrix} x + \begin{bmatrix} 0_n \\ M(q)^{-1} \end{bmatrix} u + \begin{bmatrix} \mathbf{0} \\ \Delta_d \end{bmatrix} \tag{8}$$

where 0_n is a zero matrix, and $\Delta_d = M^{-1}(q)(-C(q,\dot{q})\dot{q} - G(q) - f_{dis})$ is the uncertainty of model, $\mathbf{0}$ is a n dimensional zero vector.

When input delay and uncertainty are presented in robotic systems, (7) can be expressed as

$$\dot{x} = \begin{bmatrix} I_n \\ 0_n \end{bmatrix} x + \begin{bmatrix} 0_n \\ M(q)^{-1} \end{bmatrix} u(t-l_p) + \begin{bmatrix} \mathbf{0} \\ \Delta_d \end{bmatrix} \tag{9}$$

where $l_p > 0$ is the delay time. When $t \leq l_p$, $u(t-l_p) = 0$.

Remark 2: For the above two systems (8) and (9), the term $M^{-1}(q)G(q)$ is known, but it is included in Δ_d. The reason is that q needs to be predicted in the subsequent design of the ESO for system (9) with input delay, and errors will be generated in calculating $M^{-1}(q)$ and $G(q)$ through the predicted value of q. In order to avoid calculating the boundary of errors and ensure the consistency of the uncertainty terms in the two systems, this term is put in the uncertainty term.

For the uncertainty term, it satisfies the following assumption.

Assumption 1: Δ_d is bounded, and it has a bounded first derivative $d(t) = \frac{\mathrm{d}}{\mathrm{d}t}\Delta_d$, i.e., $\exists \delta \geq 0, \delta_d \geq 0, |\Delta_d| \leq \delta, |d(t)| \leq \delta_d$, where δ is known and δ_d is unknown.

Remark 3: This assumption is a basic premise for ESO-based control and has been applied in [31], [32], and [33]. The boundedness assumption concerning $\dot{\Delta}_d$ implies that there exists a limitation on the rate of change of the total dynamics' effects, and the change is not instantaneous. When the magnitude of $\dot{\Delta}_d$ is quite large, it requires the observer bandwidth to be sufficiently large for an accurate estimate of Δ_d. In the absence of this boundedness assumption, the rate of change in Δ_d would be unlimited, which would make Δ_d difficult to estimate. Fortunately, for robotic systems, this assumption is reasonable since $C(q,\dot{q})$ and $G(q)$ are continuous differentiable functions. However, δ_d as the boundary of $\dot{\Delta}_d$ is difficult to get. So, δ_d is assumed to be unknown in Assumption 1.

Based on the above systems and assumptions, the problems that will be studied in this article is stated as follows.

Problem 1: For the robot system (8) with dynamic uncertainty and unmeasured velocity, design a controller that renders the safety set C forward invariant.

Problem 2: For the robot system (9) with dynamic uncertainty and input delay, design a controller that renders the safety set C forward invariant.

IV. Controller Design for Uncertain Robotic Systems

This section presents a solution for Problem 1. A linear ESO is designed to estimate the dynamic model. According to estimation error, ESO-CBF is proposed and applied to the safety-critical control for robotic systems.

A. ESO Design for Robotic Systems

In accordance with the essence of CBF, the fulfillment of constraint conditions is heavily reliant upon the states and model of the system. However, in the context of a robotic system featuring an uncertain model and unmeasured state $\dot{q}$, there exists a potential challenge in utilizing CBF to ensure the satisfaction of safety constraints. To address this issue, an ESO is designed to estimate both the uncertain component of the model and $\dot{q}$.

Define $z_1 = q$, $z_2 = \dot{q}$, $z_3 = \Delta_d$, the model (8) can be transformed into extended state equation as follows:

$$\begin{cases} \dot{z_1} = z_2 \\ \dot{z_2} = M(q)^{-1}u + z_3 \\ \dot{z_3} = d(t). \end{cases} \tag{10}$$

For system (10), an ESO is constructed as follows:

$$\begin{cases} \tilde{z}_1 = z_1 - \hat{z}_1 \\ \dot{\hat{z}}_1 = \hat{z}_2 + \beta_1\omega\tilde{z}_1 \\ \dot{\hat{z}}_2 = M(z_1)^{-1}u + \hat{z}_3 + \beta_2\omega^2\tilde{z}_1 \\ \dot{\hat{z}}_3 = \beta_3\omega^3\tilde{z}_1 \end{cases} \tag{11}$$

where $\hat{z}_i$ represents the estimated value of z_i, $i = 1,2,3$, $\omega > 0$ is observer gain, $\beta_i > 0 (i = 1,2,3)$ satisfies following Hurwitz matrix.

$$\beta = \begin{bmatrix} -\beta_1 * I_n & I_n & 0_n \\ -\beta_2 * I_n & 0_n & I_n \\ -\beta_3 * I_n & 0_n & 0_n \end{bmatrix}. \tag{12}$$

For ESO (11), the estimation error is defined as $\tilde{z} = [\tilde{z}_1^T, \tilde{z}_2^T, \tilde{z}_3^T]^T$ by

$$\begin{cases} \dot{\tilde{z}}_1 = \dot{z}_1 - \dot{\hat{z}}_1 = \tilde{z}_2 - \beta_1\omega\tilde{z}_1 \\ \dot{\tilde{z}}_2 = \dot{z_2} - \dot{\hat{z}}_2 = \tilde{z}_3 - \beta_2\omega^2\tilde{z}_1 \\ \dot{\tilde{z}}_3 = \dot{z_3} - \dot{\hat{z}}_3 = d(t) - \beta_3\omega^3\tilde{z}_1. \end{cases} \tag{13}$$

Define $\varepsilon_i = \frac{\tilde{z}_i}{\omega^{i-1}} \in \mathbb{R}^n, i = 1,2,3$, the estimation error can be rewritten as $\dot{\varepsilon} = \omega\beta\varepsilon + \frac{\eta d(t)}{\omega^2}$, where $\eta = [0_n, 0_n, I_n]^T$. Solving the estimation error as $\varepsilon = e^{\omega\beta t}\varepsilon(0) + \int_0^t e^{\omega\beta(t-\vartheta)}\frac{\eta d(t)}{\omega^2}d\vartheta$.

According to [34], the estimation error is convergent and can be bounded as below for $k = 1, \ldots, 3n$.

$$|\varepsilon_k| \leq \phi(k,t) = |[e^{\omega\beta t}\varepsilon(0)]_k| + \frac{\delta}{\omega^2}|[e^{\omega\beta t}\eta]_k|. \tag{14}$$

Since β is a Hurwitz matrix, there exists a finite time $T_d > 0$ such that estimation error converge to $|\varepsilon_k| \leq \frac{1}{\omega^{3n+1}}\sum_{k=1}^{3n}|\varepsilon_k(0)| + \frac{\delta}{\omega^{3n+3}}$.

Remark 4: For estimating the uncertainty and unavailable states, various forms of ESO have been previously proposed such as classic nonlinear ESO and adaptive ESO [24]. Compared to these ESO methods, linear ESO is one of the most convenient methods for implementation, and it requires fewer parameters to design. Additionally, the real-time estimation error is required for the following design of ESO-CBF, and the estimation error of linear ESO is easier to derive than other ESO methods from the above procedure. Thus, the simpler linear ESO is used to estimate states and uncertainty.

Remark 5: Evidently, the boundary of observation error exhibits an inverse relationship with ω. Excessive amplification can diminish the estimation error, but at the expense of expanding the observation bandwidth and introducing high-frequency noise. Conversely, a minute gain amplification can increase the estimation error. Therefore, the selection of ω should balance the noise resistance ability and estimation error according to the actual situation.

B. ESO-Based CBF

Although the estimated states $\hat{x} = [\hat{z}_1^T, \hat{z}_2^T]^T$ are acquired through the utilization of ESO (11), the estimation error can potentially result in a breach of safety constraints. Therefore, the ensuing discussion will focus on elucidating the method employed to ensure the forward invariance of the safe set C by leveraging the estimated states and model.

In accordance with (14), it is apparent that the estimation error is confined within the limits of a nonincreasing function, which is related to δ. Consequently, the estimation error can be represented as $\|x - \hat{x}\| \leq \gamma(\delta, t)$. Based on this condition, the ESO-CBF is formulated to ensure the forward invariance of the safe set C.

Drawing inspiration from [16, Lemma 4], the ESO-CBF is defined as follows.

Definition 5: A continuous differentiable function $h(x)$ is ESO-CBF for uncertain system (8) with an ESO (11) of estimation bound $\gamma(\delta, t)$, if there exists a class $\mathcal{K}$ function $\alpha(\cdot)$ such that

$$L_{\bar{f}}\hat{h}(\hat{x}) + L_{\bar{g}}\hat{h}(\hat{x})u + \alpha(\hat{h}(\hat{x})) \geq 0 \tag{15}$$

where $\hat{h}(\hat{x}) = h(\hat{x}) - \bar{h}_\gamma(t)$, $\bar{h}_\gamma(t) = \sup\{h(x) : \|x - x^0\| \leq \gamma(\delta, t), x^0 \in h^{-1}(\{0\})\}$, $L_{\bar{f}}\hat{h}(\hat{x})$ and $L_{\bar{g}}\hat{h}(\hat{x})$ denote the Lie derivations of $\hat{h}(\hat{x})$ along $\bar{f}$ and $\bar{g}$ as shown below, respectively.

$$\bar{f} = \begin{bmatrix} \hat{z}_2 + \beta_1\omega\tilde{z}_1 \\ \hat{z}_3 + \beta_2\omega^2\tilde{z}_1 \end{bmatrix}, \ \bar{g} = \begin{bmatrix} 0_n \\ M(z_1)^{-1} \end{bmatrix}.$$

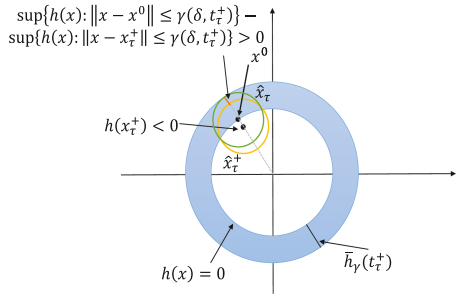

Fig. 2. Relationship between $h(x)$ and $h(\hat{x})$ in case of $h(x) = x_1^2 + x_2^2 - r^2$. The yellow circle has x_τ^+ as its center, $\gamma(\delta, t_\tau^+)$ as its radius, and the inner region represents $\|x - x_\tau^+\| \leq \gamma(\delta, t_\tau^+)$. The green circle has a x^0 as its center, $\gamma(\delta, t_\tau^+)$ as its radius, and the inner region represents a part of $\|x - x^0\| \leq \gamma(\delta, t_\tau^+)$. The red line presents $sup\{h(x) : \|x - x_\tau^+\| \leq \gamma(\delta, t_\tau^+)\} < sup\{h(x) : \|x - x^0\| \leq \gamma(\delta, t_\tau^+)$for some $x^0 \in h^{-1}(0)\}$.

The subsequent theorem illustrates the utilization of ESO-CBF to ensure the safety of a system with uncertain model.

Theorem 1: Given a continuous differentiable function $h(x)$ and a corresponding set C defined as (3), if $h(x)$ is an ESO-CBF, and the initial state $\hat{x}_0$ satisfies $\hat{h}(\hat{x}_0) > 0$, then the following Lipschitz continuous control input renders set C forward invariant.

$$u \in \{u \in U : L_{\bar{f}}\hat{h}(\hat{x}) + L_{\bar{g}}\hat{h}(\hat{x})u + \alpha(\hat{h}(\hat{x})) \geq 0\}. \tag{16}$$

Proof: As $h(x)$ is an ESO-CBF, it follows that (15) is satisfied. According to the definition of CBF, when (15) holds, the function $\hat{h}(\hat{x})$ is a CBF. In addition, the initial state $\hat{x}_0$ satisfies $\hat{h}(\hat{x}_0) > 0$. Thus, the set $C_\gamma = \{\hat{x} : \hat{h}(\hat{x}) \geq 0\}$ is rendered forward invariant based on Lemma 1, i.e., $h(\hat{x}) \geq \bar{h}_\gamma(t)$ holds for all $t > 0$. The forward invariance of safe set C can be proven through contradiction. Suppose that $x \notin C$ for some t. Given the continuity of x, there must exist a moment $t_\tau \in [0, t]$ where $h(x_\tau) = 0$ holds, and at the subsequent moment $t_\tau^+ \in [0, t]$, $h(x_\tau^+) < 0$ holds. The state x_τ, x_τ^+ satisfy $\|x_\tau - \hat{x}_\tau\| \leq \gamma(\delta, t_\tau)$ and $\|x_\tau^+ - \hat{x}_\tau^+\| \leq \gamma(\delta, t_\tau^+)$, respectively. Since $x_\tau \in h^{-1}(0)$, the following inequality arises:

$$\begin{aligned} h(\hat{x}_\tau) &\leq sup\{h(x) : \|x - x_\tau\| \leq \gamma(\delta, t_\tau)\} \\ &\leq sup\{h(x) : \|x - x^0\| \leq \gamma(\delta, t_\tau) \text{ for some } x^0 \in h^{-1}(0)\}. \end{aligned} \tag{17}$$

For x_τ^+, the following inequality exists:[1]

$$\begin{aligned} h(\hat{x}_\tau^+) &\leq sup\{h(x) : \|x - x_\tau^+\| \leq \gamma(\delta, t_\tau^+)\} \\ &< sup\{h(x) : \|x - x^0\| \leq \gamma(\delta, t_\tau^+) \text{ for some } x^0 \in h^{-1}(0)\}. \end{aligned} \tag{18}$$

Based on above inequalities, if $x \notin C$, the case $h(\hat{x}) < \bar{h}_\gamma(t)$ exists, which contradicts the condition $h(\hat{x}) \geq \bar{h}_\gamma(t_\tau)$ for all $t > 0$. Therefore, $x \in C$ for all t. The forward invariance of safe set C is proved. ■

[1] An example of a 2-D $x = [x_1, x_2]^T$ is shown in Fig. 2.

When the relative degree of $\hat{h}(\hat{x})$ is $m > 1$, the ESO-CBF is extended to ESO-HOCBF. First, a sequence of functions $\hat{\psi}_i(\hat{x})(i = 0, 1, \ldots, m)$ are defined as $\hat{\psi}_0(\hat{x}) = \hat{h}(\hat{x})$ and $\hat{\psi}_i(\hat{x}) = \dot{\hat{\psi}}_{i-1}(\hat{x}) + \alpha_i(\hat{\psi}_{i-1}(\hat{x})), i \in \{1, \ldots, m\}$, where $\alpha_i(\cdot)$ denotes $(m-i)^{th}$ order differentiable class $\mathcal{K}$ function. The corresponding sets of above functions are as follows:

$$\hat{C}_i = \{\hat{x} \in \mathbb{R}^n : \hat{\psi}_{i-1}(\hat{x}) \geq 0\}, i \in \{1, \ldots, m\}. \tag{19}$$

Based on the above functions and sets, ESO-HOCBF is defined as follows.

Definition 6: For the system (8) with relative degree m and the corresponding estimate model (11), $h(x)$ is an ESO-HOCBF for system (8), if there exist $(m-i)th$ order differentiable class $\mathcal{K}$ functions $\alpha_i, i \in \{1, \ldots, m-1\}$, and a class $\mathcal{K}$ function α_m such that $\hat{\psi}_m(\hat{x}) \geq 0$.

According to Theorem 1 and Lemma 2, if initial states $\hat{x}_0 \in \hat{C}_1 \cap \cdots \cap \hat{C}_m$ and $h(x)$ is an ESO-HOCBF, the Lipschitz continuous control input $u \in K_s(\hat{x}) = \{u \in U : \dot{\hat{\psi}}_m(\hat{x}) \geq 0\}$ renders the set C forward invariant.

C. ESO-CBF Based Control Police for Robotic Systems

To address Problem 1, the proposed ESO-CBF is applied to the robotic system with uncertain model for safety-critical control. Taking into account the dynamics model of the robot (8) and the designed ESO (11), when the safety constraint is defined as $h(q) \geq 0$, it becomes feasible to construct a QP to realize safety-critical control.

First, a new safety constraint is constructed based on the estimation error of ESO. The estimation error is expressed as follows:

$$\|x - \hat{x}\| \leq \sqrt{\sum_{k=1}^{n} \phi(k,t)^2 + \omega^2 \sum_{k=n+1}^{2n} \phi(k,t)^2}. \tag{20}$$

Let $\gamma(\delta, t) = \sqrt{\sum_{k=1}^{n} \phi(k,t)^2 + \omega^2 \sum_{k=n+1}^{2n} \phi(k,t)^2}$, the new safety constraint is constructed as $\hat{h}(\hat{z}_1) = h(\hat{z}_1) - \bar{h}_\gamma$.

Remark 6: $\gamma(\delta, t)$ is related to $\varepsilon(0) = [\tilde{z}_1(0), \tilde{z}_2(0)/\omega, \tilde{z}_3(0)/\omega^2]^T$. For robotic system, the initial value of $\dot{q}$ usually is 0, and the uncertain part is bounded by δ. So $\tilde{z}_1(0) = q(0) - \hat{z}_1(0)$, $\tilde{z}_2(0) = -\hat{z}_2(0)$, and $\tilde{z}_3(0) \leq [\delta + \hat{z}_3(0)_1, \ldots, \delta + \hat{z}_3(0)_n]^T$.

It is evident that the relative degree of $\hat{h}(\hat{z}_1)$ is 2, indicating that ESO-HOCBF is employed to ensure the satisfaction of the constraint $h(q) \geq 0$. To achieve this, two functions are defined as $\hat{\psi}_1 = \dot{\hat{h}}(\hat{z}_1) + k_1\hat{h}(\hat{z}_1)$ and $\hat{\psi}_2 = \dot{\hat{\psi}}_1 + k_2\hat{\psi}_1$, where $k_1 > 0$ and $k_2 > 0$ are parameters of the class $\mathcal{K}$ functions. Subsequently, the following QP subject to ESO-HOCBF is utilized to accomplish safety-critical control.

$$\begin{aligned} u^* &= \arg\min_u \|u - u_{nom}\|^2 \\ \text{s.t.} & L_{\hat{f}}^2\hat{h}(\hat{z}_1) + L_{\bar{g}}L_{\hat{f}}\hat{h}(\hat{z}_1)u + (k_1+k_2)L_{\hat{f}}\hat{h}(\hat{z}_1) \\ & + k_1k_2\hat{h}(\hat{z}_1) \geq 0, \\ & u_{\min} \leq u \leq u_{\max}. \end{aligned} \tag{21}$$

Remark 7: The design of the nominal controller remains unaffected by safety constraints, emphasizing its primary objective of achieving precise tracking of the predefined trajectory. Numerous research studies have been conducted to address the tracking performance of robotic systems with uncertain dynamic models. Among these approaches, the PID controller stands out as a convenient and widely used method for implementation. Therefore, in this article, a PID controller is employed as the nominal controller.

The control input derived from solving the aforementioned QP ensures the fulfillment of the safety constraint $h(q) \geq 0$ for all $t \geq 0$. Consequently, Problem 1, has been effectively addressed and resolved.

V. Controller Design for Uncertain Robotic Systems With Input Delay

In this section, a solution is proposed for Problem 2. First, ESO with a predictor is designed and the estimation error boundary is derived. Then, based on the estimation error, ESO-CBF is used to construct QP to obtain the control input and realize the safety-critical control.

A. Predictive ESO Design for Robotic Systems

For the robotic system (9) with input delay, if the ESO (11) is still used to estimate the model, there will exist a time mismatch in the real states and estimated states. Specifically, when solving for the control input at time t, the estimated state $\hat{z}_1(t)$ from the ESO (11) should correspond to the real state $q(t + l_p)$. However, the value of $q(t + l_p)$ cannot be directly obtained at time t. To address this issue, a predictor is employed to estimate $q(t + l_p)$, and the predicted value $z_p(t)$ is obtained as $z_p(t) = q(t) + \int_{t-l_p}^{t} \dot{\hat{z}}_1(\vartheta)d\vartheta$.

Following the prediction of the system states, an ESO based on $z_p(t)$ is designed as follows:

$$\begin{cases} \bar{z}_1 = z_p(t) - \hat{z}_1 \\ \dot{\hat{z}}_1 = \hat{z}_2 + \beta_1\omega\bar{z}_1 \\ \dot{\hat{z}}_2 = M(z_p)^{-1}u + \hat{z}_3 + \beta_2\omega^2\bar{z}_1 \\ \dot{\hat{z}}_3 = \beta_3\omega^3\bar{z}_1. \end{cases} \tag{22}$$

The corresponding estimation error is shown as follows:

$$\begin{cases} \dot{\tilde{z}}_1 = \tilde{z}_2 - \beta_1\omega(\tilde{z}_1 - \xi(t)) \\ \dot{\tilde{z}}_2 = (M(z_1)^{-1} - M(z_p)^{-1})u + \tilde{z}_3 - \beta_2\omega^2(\tilde{z}_1 - \xi(t)) \\ \dot{\tilde{z}}_3 = d(t) - \beta_3\omega^3(\tilde{z}_1 - \xi(t)) \end{cases} \tag{23}$$

where $\xi(t)$ represents the error between the predicted value $z_p(t)$ and the real state $q(t + l_p)$. It is expressed as $\xi(t) = q(t + l_p) - z_p(t) = \tilde{z}_1(t) - \tilde{z}_1(t - l_p)$.

The following theorem is presented to demonstrate the convergence of the PESO and establish the boundary of the estimation error:

Theorem 2: There exists observer gain $\omega > 0$ such that the estimation error shown by (23) converges and the boundary of

estimation error satisfies following for all $t \geq T_d$

$$\|\tilde{z}\| \leq \frac{2\lambda_{\max}(Q)((\delta_d+\bar{M}_\delta\omega)/\omega^2+\omega\beta_m\|\varepsilon(0)\|)}{\omega(1-\lambda_{\max}(Q)\beta_m)}\sqrt{\frac{\lambda_{\max}(Q)}{\lambda_{min}(Q)}}$$

where $\beta_m = \max(\beta_1, \beta_2, \beta_3)$, Q is a positive matrix and satisfies $\beta Q + Q\beta^T = -I$, $\lambda_{\max}(Q)\beta_m < 1$, $\bar{M}_\delta = (\frac{1}{\mu_1} - \frac{1}{\mu_2})\max(\|u_{\max}\|, \|u_{\min}\|)$.

Proof: Define $\varepsilon_i = \frac{\tilde{z}_i}{\omega^{i-1}}, i = 1, 2, 3$, $M_\delta = (M(z_1)^{-1} - M(z_p)^{-1})$, (23) can be rewritten as follows:

$$\dot{\varepsilon} = \omega\beta\varepsilon + \omega\bar{\beta}\xi + \eta d(t)/\omega^2 + \eta_2 M_\delta u/\omega \tag{24}$$

where $\bar{\beta} = [\beta_1 * I_n, \beta_2 * I_n, \beta_3 * I_n]^T$, $\eta_2 = [0_n, I_n, 0_n]^T$ Define a positive definite function $V(\varepsilon) = \varepsilon^T Q\varepsilon$, which satisfies $\lambda_{\min}(Q)\|\varepsilon\|^2 \leq V(\varepsilon) \leq \lambda_{\max}(Q)\|\varepsilon\|^2$. The derivative of $V(\varepsilon)$ is

$$\dot{V}(\varepsilon) = -\omega\varepsilon^T\varepsilon + 2\omega\varepsilon^T Q\bar{\beta}\xi + \frac{2\varepsilon^T Q(\eta d(t) + \eta_2 M_\delta\omega)}{\omega^2}. \tag{25}$$

Then, according to $\|d(t)\| \leq \delta_d$ and Property 1

$$\|\varepsilon^T Q\bar{\beta}\xi\| \leq \lambda_{\max}(Q)\beta_m\|\varepsilon\|(\|\varepsilon\| + \|\varepsilon(t-l_p)\|),$$
$$\|\varepsilon^T Q\eta d(t)\| \leq \|\varepsilon\|\|Q\|\|\eta\| \leq \lambda_{\max}(Q)\|\varepsilon\|\delta_d,$$
$$\|M_\delta u\| \leq \bar{M}_\delta = \left(\frac{1}{\mu_1} - \frac{1}{\mu_2}\right)\max(\|u_{\max}\|, \|u_{\min}\|).$$

Substituting the above two inequalities into (25)

$$\begin{aligned}\dot{V}(\varepsilon) &\leq W(\|\varepsilon\|)\\ &= 2\lambda_{\max}(Q)\|\varepsilon\|\left[\omega\beta_m\|\varepsilon(t-l_p)\|\right.\\ &\quad\left.+(\delta_d+\bar{M}_\delta\omega)/\omega^2\right] - (\omega - \omega\lambda_{\max}(Q)\beta_m)\|\varepsilon\|^2.\end{aligned}$$

When the following inequalities, $W(\|\varepsilon\|) < 0$:

$$\lambda_{\max}(Q)\beta_m < 1,$$
$$\|\varepsilon\| \geq \rho = \frac{2\lambda_{\max}(Q)\left[(\delta_d+\bar{M}_\delta\omega)/\omega^2 + \omega\beta_m\|\varepsilon(t-l_p)\|\right]}{\omega - \omega\lambda_{\max}(Q)\beta_m}.$$

According to Lyapunov-like theorem for uniform boundedness and ultimate boundedness (see [26, Theorem.18]), there exists a finite time T_d such that $\|\tilde{z}\|$ decreasing before time to T_d. When $t \geq T_d$, $\|\tilde{z}\| \leq \|\varepsilon\| \leq \kappa_1^{-1}(\kappa_2(\rho)) \leq \frac{2\lambda_{\max}(Q)((\delta_d+\bar{M}_\delta\omega)/\omega^2+\omega\beta_m\|\varepsilon_0\|)}{\omega(1-\lambda_{\max}(Q)\beta_m)}\sqrt{\frac{\lambda_{\max}(Q)}{\lambda_{\min}(Q)}}$. ■

B. Controller Synthesis for Robotic Systems

When input-delayed robotic system (9) has constraint $h(q) \geq 0$, a QP subject to ESO-CBF is constructed for safety-critical control.

The estimation error of states can be obtained by solving (24)

$$\varepsilon = e^{\omega\beta t}\varepsilon(0) + \int_0^t e^{\omega\beta(t-\vartheta)}\left(\frac{\eta d(t)}{\omega^2} + \frac{\eta_2 M_\delta}{\omega} + \omega\bar{\beta}\xi(\vartheta)\right)d\vartheta.$$

According to Theorem 2, the estimation error is convergent. So, $\|\xi\| \leq \|\varepsilon(t)\| + \|\varepsilon(t-l_p)\| \leq 2\|\varepsilon(0)\|$. Then, the estimation error can be bounded as follows:

$$\begin{aligned}|\varepsilon_k| &\leq \phi_p(k,t) = |[e^{\omega\beta t}\varepsilon(0)]_k|\\ &\quad + \frac{1}{\omega^2}|[e^{\omega\beta t}(\delta\eta + M_\delta\omega\eta_2)]_k| + 2\|\varepsilon(0)\||[e^{\omega\beta t}\bar{\beta}]_k|\end{aligned} \tag{26}$$

for $k = 1, \ldots, 3n$. According to Assumption 1, the initial estimation error of PESO is related to delay time l_p and can be bounded as follows:

$$\begin{cases}\tilde{z}_1(0) & \leq q(0) + [\frac{1}{2}\delta l_p^2 - \hat{z}_1(0), \ldots, \frac{1}{2}\delta l_p^2 - \hat{z}_1(0)_n]^T\\ \tilde{z}_2(0) & \leq [\delta l_p - \hat{z}_2(0)_1, \ldots, \delta l_p - \hat{z}_2(0)_n]^T\\ \tilde{z}_3(0) & \leq [\delta + \hat{z}_3(0)_1, \ldots, \delta + \hat{z}_3(0)_n]^T.\end{cases}$$

Remark 8: In accordance with Theorem 1, the safety of robotic systems with input delay can be assured if the constraint $\hat{h}(\hat{z}_1) = h(\hat{z}_1) - \bar{h}\gamma \geq 0$ holds for all $t \geq 0$. By (26), the estimation error is bounded as $\gamma(\delta, t) = \sqrt{\sum_{k=1}^{n}\phi_p(k,t)^2 + \omega^2\sum_{k=n+1}^{2n}\phi_p(k,t)^2}$. Subsequently, the control input is determined by solving QP (21) at each interval. Through this approach, the implementation of safety-critical control for robotic systems with input delay is accomplished.

Remark 9: It should be noted that $\hat{h}(\hat{z}_1)$ is influenced by the estimation error of the PESO, which is directly proportional to the delay l_p. Consequently, a longer delay leads to a larger estimation error, thereby resulting in a more conservative safety constraint defined by $\hat{h}(\hat{z}_1)$. In the case of robotic systems, input delays typically range in the milliseconds [35], and the conservatism introduced by this delay in the safety constraint $\hat{h}(\hat{z}_1)$ is generally acceptable. However, for robotic systems with significantly longer delays, future research will investigate modifications to the PESO design to mitigate the estimation error and reduce the conservatism of the safety constraint.

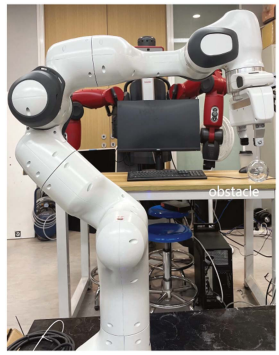

Fig. 3. Experiment platform: A Franka Emika Panda manipulator with an obstacle.

VI. Experiment on Franka Emika Robot

This section presents a physical experiment designed to validate the proposed framework, including a seven-DOF Franka Emika Panda manipulator and a spherical obstacle with a radius of 2 cm, as depicted in Fig. 3. The experiment is executed utilizing the Franka Control Interface (FCI) facilitated by libfranka on the Ubuntu 20.04 LTS operating system.

To provide further clarity, the experiment designs a specific task: achieving obstacle avoidance with the manipulator's end-effector while tracking a predetermined trajectory. The obstacle is positioned at (0.295, 0.038, 0.458) in the base frame, allowing the obstacle avoidance constraint to be characterized by a continuous differentiable function $h(q) : \mathbb{R}^7 \to \mathbb{R}$

$$h(q) = (x(q) - 0.295)^2 + (y(q) - 0.038)^2 + (z(q) - 0.458)^2 - r^2 \tag{27}$$

where $x(q)$, $y(q)$, and $z(q)$ are the coordinates of end-effector. The real-time position information of end-effector can be directly accessed by FCI. The associated videos for demonstration can be found at https://youtu.be/o5szROzJbTk.

The initial joint states are given by $q(0) = [0, -\pi/4, 0, -3\pi/4, 0, 3\pi/4, \pi/4]^T$rad. The external disturbances is $f_{dis} = [6, 6, 6, 6, 2, 2, 2]$. In accordance with the parameter specification of the Franka Emika robot, the joint accelerations are constrained within the limits of $\ddot{q}_{\max} = -\ddot{q}_{\min} = [15, 7.5, 10, 12.5, 15, 20, 20]$rad/s^2. Moreover, the joint torques are subject to the constraints that $u_{\max} = -u_{\min} = [87, 87, 87, 87, 12, 12, 12]^T$Nm, and sampling time is $t_{k+1} - t_k = 0.001$ s. If the aforementioned limitations are not satisfied, the manipulator's motion will be terminated. Due to $\Delta_d = \ddot{q} - M(q)^{-1}u$, the boundary of model uncertainty δ can be calculated as $\delta = \|1/\mu_1 u_{\max} + \ddot{q}_{\max}\|$, where $\mu_1 = 1$.

For the robotic system without input delay, the parameters of ESO are set as $\beta_1 = 3$, $\beta_2 = 3$, $\beta_3 = 1$. In order to evaluate the impact ω on estimation error, four distinct values of ω are set as follows:

$$\begin{cases} \omega_1 = [20, 10, 20, 10, 5, 5, 5]^T \\ \omega_2 = [25, 15, 25, 15, 10, 10, 10]^T \\ \omega_3 = [30, 20, 30, 20, 15, 15, 15]^T \\ \omega_4 = [35, 25, 35, 25, 20, 20, 20]^T. \end{cases}$$

Fig. 4(a)–(c) depict the estimation error of q, $\dot{q}$, and Δ_d under the influence of ω_1, respectively. It is discernible that the error gradually converges and remains confined within a delimited range. Fig. 4(d) presents the fourth component of the uncertainty estimation error across varying values of ω. Although only one component of the estimation error is showcased due to page constraint, it sufficiently illustrates the impact of ω on estimation error. Fig. 4(d) suggests that augmenting ω can expedite the speed of error convergence, but excessively large ω values will amplify the fluctuation of the estimation result.

In order to accomplish the obstacle avoidance task, a new constraint function $\hat{h}(\hat{z}_1)$ is formulated based on the estimation error.

$$\begin{aligned} \hat{h}(\hat{z}_1) = &(x(\hat{z}_1) - 0.295)^2 + (y(\hat{z}_1) - 0.038)^2 \\ &+ (z(\hat{z}_1) - 0.0458)^2 - (r + \gamma(\delta, t))^2 \geq 0 \end{aligned} \tag{28}$$

where $\gamma(\delta, t)$ is calculated as (20). The parameters of HOCBF are set as $k_1 = 10$ and $k_2 = 5$.

As $\hat{h}(\hat{z}_1)$ is related to δ, four different values of δ are assigned as $\delta_1 = 203, \delta_2 = 189, \delta_3 = 178, \delta_4 = 167$ to evaluate the impact of δ on performance of the proposed control method. These

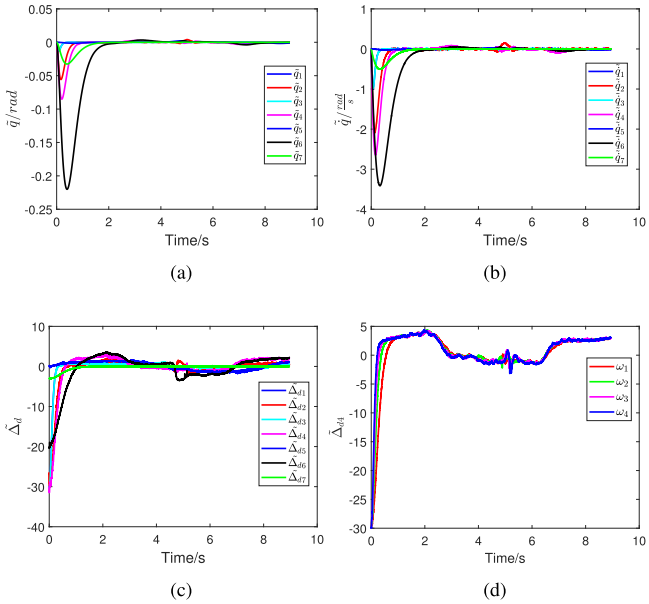

Fig. 4. Estimation error of states by ESO. (a) The estimation error of q. (b) The estimation error of $\dot{q}$. (c) The estimation error of Δ_d. (d) The fourth component of estimation error of Δ_d with different ω.

different values of δ are determined by selecting diverse control input constraints. To achieve the aforementioned δ values, four sets of control input constraints are established.

$$\begin{cases} u^1_{\max} = [87, 87, 87, 87, 12, 12, 12]\text{Nm} \\ u^2_{\max} = [80, 80, 80, 80, 10, 10, 10]\text{Nm} \\ u^3_{\max} = [75, 75, 75, 75, 8, 8, 8]\text{Nm} \\ u^4_{\max} = [70, 70, 70, 70, 5, 5, 5]\text{Nm}. \end{cases}$$

Fig. 5(a) presents the control input obtained from QP (21) for δ_1. The response curves of $\hat{h}(\hat{z}_1)$ and $\psi_1(\hat{z}_1)$ are depicted in Fig. 5(b), demonstrating that both satisfy constraints. Moreover, Fig. 5(c) exhibits the trajectory of the robot driven by the proposed control method across varying values of δ. As shown in (20), an increase in δ leads to a corresponding increase in $\gamma(\delta, t)$. Notably, elevated values of $\gamma(\delta, t)$ tend to induce a more conservative control performance. This aligns with the observation in Fig. 5(c) where the control performance exhibits increased conservatism with higher δ. However, when confronted with larger δ, the conservatism can be alleviated by increasing ω. Fig. 5(d) illustrates the robot's trajectory for different ω settings when $\delta = \delta_1$. Obviously, the depicted trajectories showcase a reduction in conservatism as ω increases.

For the robotic system with input delay, the parameters of PESO are set as $\beta_1 = 3$, $\beta_2 = 3$, $\beta_1 = 1$. In order to evaluate the impact ω on estimation error, four different ω values are set as follows:

$$\begin{cases} \omega_1 = [20, 10, 20, 5, 5, 10, 10]^T \\ \omega_2 = [25, 15, 25, 10, 10, 15, 15]^T \\ \omega_3 = [30, 20, 30, 15, 15, 20, 20]^T \\ \omega_4 = [35, 25, 35, 20, 20, 25, 25]^T. \end{cases}$$

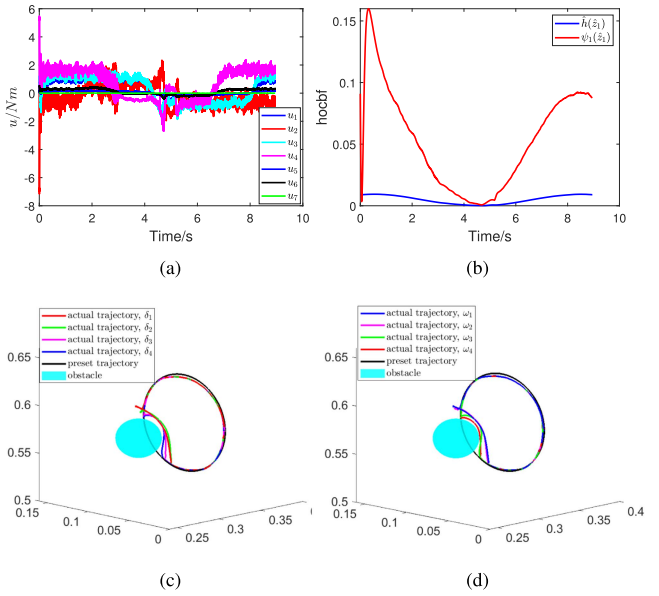

Fig. 5. Control input, constraint functions, and trajectories of end-effector. (a) The control input solved by QP (21). (b) The curves of $\hat{h}(\hat{z}_1)$ and $\psi_1(\hat{z}_1)$. (c) The preset trajectory and actual trajectory of robot end-effector with different δ. (d) The preset trajectory and actual trajectory of robot end-effector with different ω.

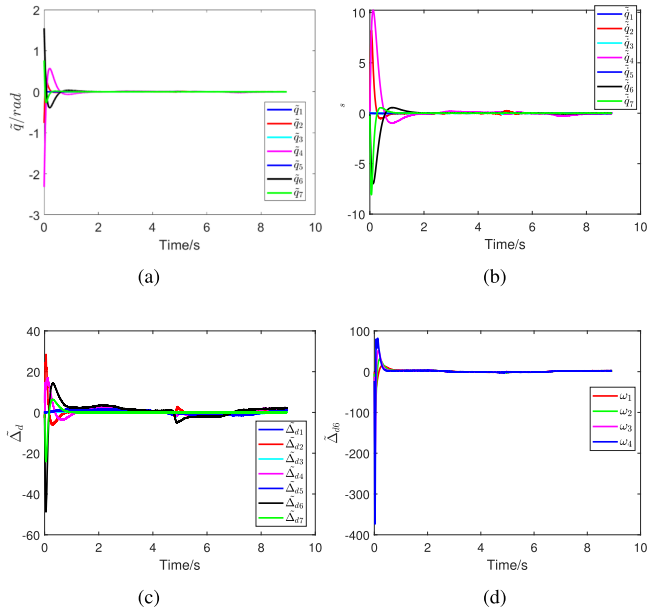

Fig. 6. Estimation error of states by PESO. (a) The estimation error of q. (b) The estimation error of $\dot{q}$. (c) The estimation error of Δ_d. (d) The sixth component of estimation error of Δ_d under different ω.

The estimation errors of q, $\dot{q}$, and Δ_d with a delay of $l_p = 0.015\,\mathrm{s}$ and ω_1 are depicted in Fig. 6(a)–(c). These plots reveal that the estimation errors converge and maintain their bounds. Additionally, Fig. 6(d) illustrates the sixth component of the uncertainty estimation error across various values of ω. Notably, the outcome bears resemblance to the findings observed in the ESO estimation error across different ω values.

With a delay of $l_p = 0.015\,\mathrm{s}$ and $\omega = \omega_1$, Fig. 7(a) showcases the control input derived from QP (21), while Fig. 7(b)

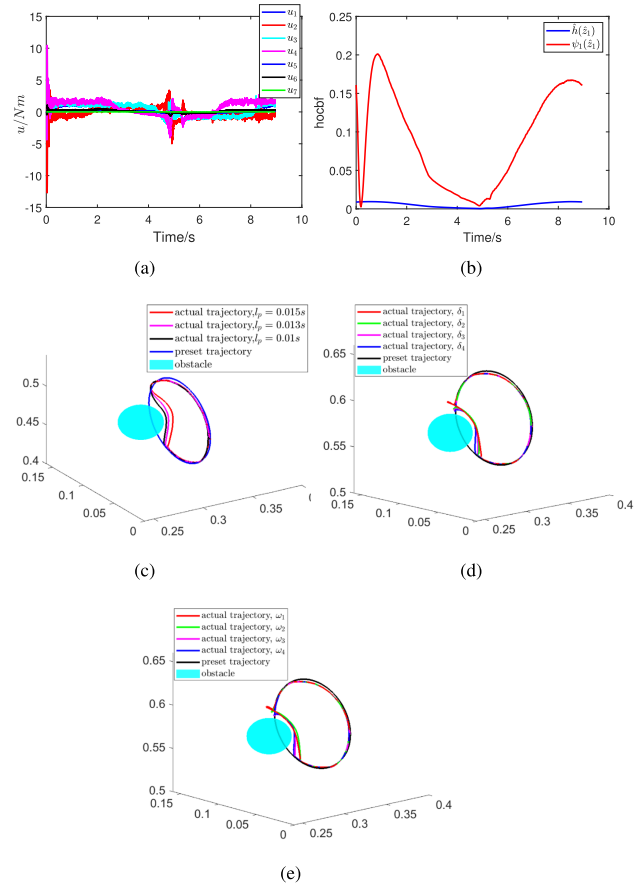

Fig. 7. Control input, constraint functions and trajectories of end-effector. (a) The control input solved by QP (21). (b) The curves of $\hat{h}(\hat{z}_1)$ and $\psi_1(\hat{z}_1)$. (c) The preset trajectory and actual trajectory of robot end-effector with different delay. (d) The preset trajectory and actual trajectory of robot end-effector with different δ. (e) The preset trajectory and actual trajectory of robot end-effector with different ω when $\delta = \delta_1$.

displays the response curves of $\hat{h}(\hat{z}_1)$ and $\psi_1(\hat{z}_1)$, both satisfying the imposed constraints. Fig. 7(c) depicts the trajectories of robot with varying delay conditions. As the delay increases, the level of constraint becomes more conservative, which aligns with the concept discussed in Remark 9 where the definition of $\hat{h}(\hat{z}_1)$ is directly proportional to the delay. With a delay of $l_p = 0.015\,\mathrm{s}$, Fig. 7(d) illustrates the robot's trajectories with different δ values to assess the impact of δ on the performance of the proposed control method. As δ increases, the control performance becomes increasingly conservative. When $\delta = \delta_1$, the trajectories are shown in Fig. 7(e) with different ω settings. Notably, the conservatism can be mitigated by appropriately increasing ω when δ is excessively large.

VII. Conclusion

To address the challenges posed by dynamic uncertainty and unmeasured joint velocity in robotic systems, a safety-critical control framework was proposed by integrating the concepts of ESO and CBF. A linear ESO was utilized to get the estimation

of system uncertainties and states, and ESO-CBF is proposed based on the estimation error to guarantee the safety constraint. Additionally, when the robotic system encounters input delays, an ESO with a predictor was introduced to estimate the model, providing the boundary for estimation error. Consequently, the proposed ESO-CBF approach could be employed to execute safety-critical control. The efficacy of this method was validated through experiments conducted on the Franka Emika Panda manipulator.

REFERENCES

[1] C. Yang, D. Huang, W. He, and L. Cheng, "Neural control of robot manipulators with trajectory tracking constraints and input saturation," *IEEE Trans. Neural Netw. Learn. Syst.*, vol. 32, no. 9, pp. 4231–4242, Sep. 2021.

[2] S. Prajna and A. Jadbabaie, "Safety verification of hybrid systems using barrier certificates," in *Proc. Int. Workshop Hybrid Syst.: Comput. Control*, 2004, pp. 477–492.

[3] X. Xu et al., "Realizing simultaneous lane keeping and adaptive speed regulation on accessible mobile robot testbeds," in *Proc. IEEE Conf. Control Technol. Appl.*, 2017, pp. 1769–1775.

[4] M. Jankovic, "Robust control barrier functions for constrained stabilization of nonlinear systems," *Automatica*, vol. 96, pp. 359–367, 2018.

[5] L. Lindemann and D. V. Dimarogonas, "Control barrier functions for multi-agent systems under conflicting local signal temporal logic tasks," *IEEE Contr. Syst. Lett.*, vol. 3, no. 3, pp. 757–762, Jul. 2019.

[6] A. D. Ames, X. Xu, J. W. Grizzle, and P. Tabuada, "Control barrier function based quadratic programs for safety critical systems," *IEEE Trans. Autom. Control*, vol. 62, no. 8, pp. 3861–3876, Aug. 2017.

[7] B. Zhang, Y. Jia, and J. Du, "Adaptive synchronization control of networked robot systems without velocity measurements," *Int. J. Robust Nonlinear Control*, vol. 28, no. 11, pp. 3606–3622, 2018.

[8] D. Huang, B. Li, Y. Li, and C. Yang, "Cooperative manipulation of deformable objects by single-leader–dual-follower teleoperation," *IEEE Trans. Ind. Electron.*, vol. 69, no. 12, pp. 13162–13170, Dec. 2022.

[9] C. Yang, G. Peng, L. Cheng, J. Na, and Z. Li, "Force sensorless admittance control for teleoperation of uncertain robot manipulator using neural networks," *IEEE Trans. Syst., Man, Cybern. Syst.*, vol. 51, no. 5, pp. 3282–3292, May 2021.

[10] Q. Nguyen and K. Sreenath, "Robust safety-critical control for dynamic robotics," *IEEE Trans. Autom. Control*, vol. 67, no. 3, pp. 1073–1088, Mar. 2022.

[11] A. J. Taylor and A. D. Ames, "Adaptive safety with control barrier functions," in *Proc. Amer. Control Conf.*, 2020, pp. 1399–1405.

[12] B. T. Lopez, J.-J. E. Slotine, and J. P. How, "Robust adaptive control barrier functions: An adaptive and data-driven approach to safety," *IEEE Contr. Syst. Lett.*, vol. 5, no. 3, pp. 1031–1036, Jul. 2020.

[13] Y. Emam, P. Glotfelter, S. Wilson, G. Notomista, and M. Egerstedt, "Data-driven robust barrier functions for safe, long-term operation," *IEEE Trans. Robot.*, vol. 38, no. 3, pp. 1671–1685, Jun. 2022.

[14] C. Zhu, Y. Jiang, and C. Yang, "Fixed-time neural control of robot manipulator with global stability and guaranteed transient performance," *IEEE Trans. Ind. Electron.*, vol. 70, no. 1, pp. 803–812, Jan. 2023.

[15] S. Dean, A. Taylor, R. Cosner, B. Recht, and A. Ames, "Guaranteeing safety of learned perception modules via measurement-robust control barrier functions," in *Proc. Conf. Robot Learn.*, 2021, pp. 654–670.

[16] A. Clark, "Control barrier functions for stochastic systems," *Automatica*, vol. 130, 2021, Art. no. 109688.

[17] N. Jahanshahi, P. Jagtap, and M. Zamani, "Synthesis of stochastic systems with partial information via control barrier functions," *IFAC-PapersOnLine*, vol. 53, no. 2, pp. 2441–2446, 2020.

[18] D. R. Agrawal and D. Panagou, "Safe and robust observer-controller synthesis using control barrier functions," *IEEE Contr. Syst. Lett.*, vol. 7, pp. 127–132, 2022.

[19] K. Garg and D. Panagou, "Robust control barrier and control Lyapunov functions with fixed-time convergence guarantees," in *Proc. IEEE Amer. Control Conf.*, 2021, pp. 2292–2297.

[20] I. Abel, M. Jankovic, and M. Krstić, "Constrained stabilization of multi-input linear systems with distinct input delays," *IFAC-PapersOnLine*, vol. 52, no. 2, pp. 82–87, 2019.

[21] I. Abel, M. Krstić, and M. Janković, "Safety-critical control of systems with time-varying input delay," *IFAC-PapersOnLine*, vol. 54, no. 18, pp. 169–174, 2021.

[22] Z. Liu, L. Yang, and N. Ozay, "Scalable computation of controlled invariant sets for discrete-time linear systems with input delays," in *Proc. IEEE Amer. Control Conf.*, 2020, pp. 4722–4728.

[23] T. G. Molnar, A. K. Kiss, A. D. Ames, and G. Orosz, "Safety-critical control with input delay in dynamic environment," *IEEE Trans. Control Syst. Technol.*, vol. 31, no. 4, pp. 1507–1520, Jul. 2023.

[24] X. Zhang, X. Zhang, W. Xue, and B. Xin, "An overview on recent progress of extended state observers for uncertain systems: Methods, theory, and applications," *Adv. Control Appl.: Eng. Ind. Syst.*, vol. 3, no. 2, 2021, Art. no. e89.

[25] F. Blanchini, "Set invariance in control," *Automatica*, vol. 35, no. 11, pp. 1747–1767, 1999.

[26] H. K. Khalil, *Nonlinear Systems.*, Englewood Cliffs, NJ, USA: Prentice-Hall, 2002.

[27] W. Xiao and C. Belta, "High order control barrier functions," *IEEE Trans. Autom. Control*, vol. 67, no. 7, pp. 3655–3662, Jul. 2022, doi: 10.1109/TAC.2021.3105491.

[28] W. Xiao, C. Belta, and C. G. Cassandras, "Adaptive control barrier functions," *IEEE Trans. Autom. Control*, vol. 67, no. 5, pp. 2267–2281, May 2022.

[29] W. Xiao, C. A. Belta, and C. G. Cassandras, "Sufficient conditions for feasibility of optimal control problems using control barrier functions," *Automatica*, vol. 135, 2022, Art. no. 109960.

[30] S. Roy, S. B. Roy, and I. N. Kar, "Adaptive–robust control of Euler-Lagrange systems with linearly parametrizable uncertainty bound," *IEEE Trans. Control Syst. Technol.*, vol. 26, no. 5, pp. 1842–1850, Sep. 2018.

[31] H. Pan, W. Sun, H. Gao, T. Hayat, and F. Alsaadi, "Nonlinear tracking control based on extended state observer for vehicle active suspensions with performance constraints," *Mechatronics*, vol. 30, pp. 363–370, 2015.

[32] R. Cui, L. Chen, C. Yang, and M. Chen, "Extended state observer-based integral sliding mode control for an underwater robot with unknown disturbances and uncertain nonlinearities," *IEEE Trans. Ind. Electron.*, vol. 64, no. 8, pp. 6785–6795, Aug. 2017.

[33] H. Castañeda, O. S. Salas-Peña, and J. de León-Morales, "Extended observer based on adaptive second order sliding mode control for a fixed wing UAV," *ISA Trans.*, vol. 66, pp. 226–232, 2017.

[34] C. Ren, X. Li, X. Yang, and S. Ma, "Extended state observer-based sliding mode control of an omnidirectional mobile robot with friction compensation," *IEEE Trans. Ind. Electron.*, vol. 66, no. 12, pp. 9480–9489, Dec. 2019.

[35] T. T. Andersen, H. B. Amor, N. A. Andersen, and O. Ravn, "Measuring and modelling delays in robot manipulators for temporally precise control using machine learning," in *Proc. IEEE Int. Conf. Mach. Learn. Appl.*, 2015, pp. 168–175.

Sihua Zhang received the M.Eng. degree in control engineering from the Beijing Institute of Technology, Beijing, China, in 2021. She is currently working toward the Ph.D. degree in control engineering with the School of Automation, Beijing Institute of Technology, Beijing, China.

Her current research interests include robotic control, CBFs, and optimal control.

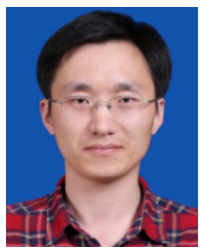

Di-Hua Zhai received the B.Eng. degree in automation from Anhui University, Hefei, China, in 2010, the M.Eng. degree in control science and engineering from the University of Science and Technology of China, Hefei, China, in 2013, and the Dr.Eng. degree in control science and engineering from the Beijing Institute of Technology, Beijing, China, in 2017.

Since 2017, he has been an Associate Professor with the School of Automation, Beijing Institute of Technology. His research interests include intelligent robot, networked robots, computer vision in robotics, artificial intelligence in medicine, switched control, and optimal control.

Juncheng Lin received the B.Eng. degree in energy and power engineering, in 2021, from the Beijing Institute of Technology, Beijing, China, where he is currently working toward the master's degree in control science and engineering with the School of Automation.

His current research interests include robotic control, CBFs, and optimal control.

Yuhan Xiong received the B.Eng. degree in automation from Shandong University, Jinan, China, in 2020, and the M.S. degree in control science and engineering from Beijing Institute of Technology, Beijing, China, in 2023. She is currently working toward the Ph.D. degree in control science and engineering with the School of Automation, Beijing Institute of Technology.

Her current research interests include robotic control, CBFs, and optimal control.

Yuanqing Xia (Senior Member, IEEE)) received the M.S. degree in fundamental mathematics from Anhui University, Hefei, China, in 1998, and the Ph.D. degree in control theory and control engineering from the Beijing University of Aeronautics and Astronautics, Beijing, China, in 2001.

From 2002 to 2003, he was a Postdoctoral Research Associate with the Institute of Systems Science, Academy of Mathematics and System Sciences, Chinese Academy of Sciences, Beijing, China. From 2003 to 2004, he was a Research Fellow with the National University of Singapore, Singapore, where he worked on variable structure control. From 2004 to 2006, he was a Research Fellow with the University of Glamorgan, Pontypridd, U.K. From 2007 to 2008, he was a Guest Professor with Innsbruck Medical University, Innsbruck, Austria. Since 2004, he has been with the Department of Automatic Control, Beijing Institute of Technology, first as an Associate Professor, then, since 2008, as a Professor. His current research interests include cloud control systems, networked control systems, robust control and signal processing, active disturbance rejection control, unmanned system control, and flight control.

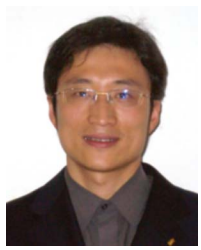

Minfeng Wei received the B.Eng. degree in automation from the Dalian University of Technology, Dalian, China, in 2000, and the M.Eng. degree in computer application from the University of Chinese Academy of Sciences, Beijing, China, in 2008.

He is currently a Research Staff with the Beijing Institute of Aerospace Automatic Control, Beijing, China. His current research interests include aerospace intelligent control.